Journal of Solid State Chemistry 181 (2008) 1899–1908

Contents lists available at ScienceDirect

Journal of Solid State Chemistry

journal homepage: www.elsevier.com/locate/jssc

Adaptable coordination of U(IV) in the 2D-(4,4) uranium oxalate network: From 8 to 10 coordinations in the uranium (IV) oxalate hydrates

L. Duvieubourg-Garela [a], N. Vigier [b], F. Abraham [a,*], S. Grandjean [b]

[a] UCCS—Equipe Chimie du Solide, UMR CNRS 8181, ENSCL-USTL, B.P. 90108, 59652 Villeneuve d'Ascq Cedex, France
[b] Laboratoire de Chimie des Actinides, CEA VALRHO/DRCP/SCPS, Bât 399 BP 17171, 30208 Bagnols sur Ceze Cedex, France

ARTICLE INFO

Article history:
Received 19 February 2008
Received in revised form
4 April 2008
Accepted 4 April 2008
Available online 25 April 2008

Keywords:
Uranium (IV) oxalates
Crystal structure
Metal oxalate framework
Uranium (IV) coordination
Thermal decomposition

ABSTRACT

Crystals of uranium (IV) oxalate hydrates, $U(C_2O_4)_2 \cdot 6H_2O$ (**1**) and $U(C_2O_4)_2 \cdot 2H_2O$ (**2**), were obtained by hydrothermal methods using two different U(IV) precursors, U_3O_8 oxide and nitric U(IV) solution in presence of hydrazine to avoid oxidation of U(IV) into uranyl ion. Growth of crystals of solvated monohydrated uranium (IV) oxalate, $U(C_2O_4)_2 \cdot H_2O \cdot (dma)$ (**3**), dma = dimethylamine, was achieved by slow diffusion of U(IV) into a gel containing oxalate ions. The three structures are built on a bi-dimensional complex polymer of U(IV) atoms connected through bis-bidentate oxalate ions forming $[U(C_2O_4)]_4$ pseudo-squares. The flexibility of this supramolecular arrangement allows modifications of the coordination number of the U(IV) atom which, starting from 8 in **1** increases to 9 in **3** and, finally increases, to 10 in **2**. The coordination polyhedron changes from a distorted cube, formed by eight oxygen atoms of four oxalate ions, in **1**, to a mono-capped square anti-prism in **3** and, finally, to a di-capped square anti-prism in **2**, resulting from rotation of the oxalate ions and addition of one and two water oxygen atoms in the coordination of U(IV). In **1**, the space between the $^2_\infty[U(C_2O_4)_2]$ planar layers is occupied by non-coordinated water molecules; in **2**, the space between the staggered $^2_\infty[U(C_2O_4)_2 \cdot 2H_2O]$ layers is empty, finally in **3**, the solvate molecules occupy the interlayer space between corrugated $^2_\infty[U(C_2O_4)_2 \cdot H_2O]$ sheets. The thermal decomposition of $U(C_2O_4)_2 \cdot 6H_2O$ under air and argon atmospheres gives U_3O_8 and UO_2, respectively.

1. Introduction

Actinide oxalates play an important role in the nuclear industry; in fact, oxalic acid is often used as precipitating agent in the nuclear fuel technology or for waste decontamination purpose or as complexing agent to adjust extracting characteristics of actinides. The knowledge of actinide oxalate properties can also contribute to model the migration of radionucleides in the environment because the most important mechanism is the complexation of radionucleides by carboxylic functional groups of bacterial humic acids [1]. Since uranium is oxidized by atmospheric oxygen into uranium (VI), the crystal chemistry of uranyl containing oxalates has been extensively studied and is rather rich [2–16]. In contrast U(IV) oxalates have been less investigated although, in some oxalate precipitating processes, U(IV) is stabilized in nitric solution, after adding an anti-nitrous agent such as hydrazinium nitrate ($N_2H_5^+$, NO_3^-) to the solution. In addition the uranium (IV) oxalate is among the most stable uranium (IV) solids. So, the knowledge of uranium (IV) oxalates is of importance. Whereas the structures of some double or triple oxalates of U(IV) with monovalent, divalent or trivalent atoms were reported [17–23], the structures of simple uranium oxalates are not known. The existence of hexa-, di-, mono-hydrated and anhydrous U(IV) oxalates has been reported. Jenkins et al. [24] and Bressat et al. [25] gave a triclinic cell, with $a = 6.388(3)$, $b = 6.388(3)$, $c = 7.881(4)$ Å, $\alpha = 91.64(1)$, $\beta = 91.64(1)$, $\gamma = 89.45(1)^\circ$, for the uranium oxalate hexahydrate $U(C_2O_4)_2 \cdot 6H_2O$ and an orthorhombic cell with face centered lattice, with $a = 10.479(3)$, $b = 9.443(3)$, $c = 8.572(3)$ Å, for the uranium oxalate dihydrate $U(C_2O_4)_2 \cdot 2H_2O$. By analogy with the neptunium analogue, Grigoriev et al. [26] propose to transform the triclinic cell of the uranium (IV) hexahydrate into a monoclinic one with parameters $a = 9.081(4)$, $b = 8.893(4)$, $c = 7.878(4)$ Å, $\beta = 92.31(2)^\circ$. Since the hexahydrate losses, at low temperature four water molecules, it is assumed that in the hexa- and di- hydrates two water molecules pertain to the inner-coordination sphere of U(IV) [27]. To explain the existence of the monohydrate, it was also assumed that one water molecule is coordinated to the uranium atom and the other is attached to the oxalate group [28]. This paper reports the crystal structure of the hexa-, the di- and the solvated mono-hydrate oxalates of U(IV) together with some characterizations of the transitions that illustrate the adaptable coordination of U(IV).

* Corresponding author. Fax: +33 3 20 43 68 14.
E-mail address: francis.abraham@ensc-lille.fr (F. Abraham).

0022-4596/$ - see front matter © 2008 Elsevier Inc. All rights reserved.
doi:10.1016/j.jssc.2008.04.010

2. Experimental

2.1. Synthesis

2.1.1. $U(C_2O_4)_2 \cdot 6H_2O$ (**1**)

A mixture of uranium oxide U_3O_8 (84.2 mg, 0.1 mmole) and oxalic acid (45 mg, 0,5 mmole) was added to 1 mL of 0.2 M hydrazine solution and to 5 mL of demineralised water and placed in a Teflon-lined stainless-steel 23-mL autoclave at 80 °C under autogenous pressure. Few green single crystals of **1** (Fig. 1a) embedded in U_3O_8 powder were obtained within 3 days. Let us point out that the use of U^{4+} solution instead of U_3O_8 led, in the same conditions, to rapid precipitation of powdered $U(C_2O_4)_2 \cdot 6H_2O$.

2.1.2. $U(C_2O_4)_2 \cdot 2H_2O$ (**2**)

Single crystals of **2** (Fig. 1b), accompanied by poor quality single crystals of **1**, were grown starting from the same solution of oxalic acid (0.063 g, 5 mmole) in a 0.065 M solution of U^{4+} (5 mL, 0.325 mmole) stabilized with a 0.2 M hydrazine solution (1 mL, 0.2 mmole) placed in a Teflon-lined stainless-steel 23-mL autoclave at 120 °C under autogenous pressure during a longer time (3 days).

2.1.3. $U(C_2O_4)_2 \cdot H_2O \cdot (dma)$ (**3**)

Single crystals of **3** (Fig. 1c) were obtained by the slow diffusion of the cations U^{4+} through TEOS gel impregnated with oxalic acid. For the TEOS gel preparation, exactly measured volumes of TEOS (2.5 mL) and ethanol (1.5 mL) were mixed. To the mixture was slowly added a solution of HNO_3, 3 M (1 mL), oxalic acid, 1 M (1.5 mL) and distilled water (1 mL). The heating of this mixture at 60 °C for 24 h resulted in a gel formation. When a mixture of 4 mL of a 0.065 M aqueous solution of U^{4+} and 1 mL of 0.2 M dimethylamine solution is slowly added on the gel, colorless plate-shaped crystals of **3** slowly form inside the gel after 2 days.

2.2. Single-crystal data collection

The single crystal diffraction intensities were measured at 293 K on a AXS BRUKER X8 APEX II diffractometer for **1** and **2** and at 100 K on a AXS BRUKER SMART APEX II diffractometer for **3**. The diffractometers were equipped with a fine-focus Mo-target X-ray tube ($\lambda = 0.71073$ Å) operated at 2000 W power. The detectors were placed at a distance of 5.41 cm from the crystal and the intensities were measured under the conditions given in Table 1 and extracted from the collected frames using the program SaintPlus 6.02 [29]. The structure resolutions and refinements were performed with the SHELXTL software package [30]. The lattice parameters were refined from the complete data set and an empirical absorption correction was applied for the three compounds [31]. The heavy atoms were located using the direct methods, while the remaining atoms were found from successive Fourier map analyses. The location of the H atoms of water molecules was not determined because of the presence of very heavy atoms and important thermal agitation of water molecules. The atomic positions and the anisotropic displacement parameters for all atoms, except the solvate molecule atoms in **3** for which isotropic displacement parameters were included in the last cycles of refinement.

The atomic positional parameters and displacement parameters are given in Tables 2–4 for compounds **1**, **2** and **3**, respectively. For compound **1**, the high residues of electronic densities are located at about 0.8 Å of the uranium atom as often observed in structures containing heavy atoms.

2.3. Powder synthesis and powder X-ray diffraction

Very well crystallized powder of **1** was obtained by hydrothermal synthesis from oxalic acid (0.063 g, 5 mmole) dissolved in a 0.065 M aqueous solution of U^{4+} (5 mL, 0.325 mmole) added with a 0.2 M hydrazine solution (1 mL, 0.2 mmole) maintained under autogenous pressure at 80 °C during 4 h. Finally, powder of **2** was obtained by heating the powder of compound **1** at 100 °C for 1 h.

For unit cell parameters refinement, powder X-ray diffraction data have been collected with a Bruker D8 $\theta/2\theta$ diffractometer equipped by Cu$K\alpha$ radiation, using Bragg-Brentano geometry, in steps of 0.02° and a counting time of 30 s per step, within an angular range from 5 to 110° in 2θ. The unit cell parameters were refined from powder diffraction pattern using the Rietveld method [32,33]. The refinement was carried out using the "*pattern matching*" option of the Fullprof program [34], where only the profile parameters (cell dimensions, peak shapes, background, zero point correction and symmetry) have been refined. The peak shape was described by a pseudo-Voigt function with an asymmetry correction at low angles. In order to describe the angular dependence of the peak full-width at half-maximum (H), the formulation of Caglioti et al. [35] was used: $H^2 = U\tan^2\theta + V\tan\theta + W$ where U, V and W parameters were refined in the process.

2.4. Thermal analysis

Simultaneous thermogravimetric (TG) and differential thermal (DT) analyses were performed at a constant heating rate of 5 °C/min up to 700 °C under a N_2–O_2 gas atmosphere (N_2:O_2 = 4:1 by vol) using a SETARAM 92 thermal analysis system. The evolved gases were examined by a PFEIFFER VACCUM GSD-301 mass spectrometer (MS). High-temperature X-ray diffraction (HTXRD) was performed under the same gas atmosphere with a Bruker D8 θ/θ powder diffractometer using Cu$K\alpha$ radiation and equipped with a HTK 1200 Anton Parr device and a Vantec detector. The

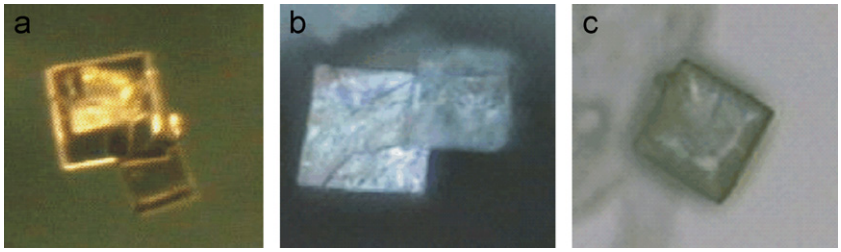

Fig. 1. Pictures of single crystals in the form of square plates of (a) $U(C_2O_4)_2 \cdot 6H_2O$, (b) $U(C_2O_4)_2 \cdot 2H_2O$ obtained by mild hydrothermal syntheses and (c) $[U(C_2O_4)_2 \cdot H_2O](C_2NH_5)$ grew using a gel method.

Table 1
Crystal data and structure refinement for $[U(C_2O_4)_2]\cdot 6H_2O$, **1** $[U(C_2O_4)_2\cdot 2H_2O]$, **2** and $[U(C_2O_4)_2\cdot H_2O](C_2NH_7)$, **3**

Compound	**1**	**2**	**3**
Empirical formula	$UC_4O_{14}H_{12}$	$UC_4O_{10}H_4$	$UC_6O_9N_1H_9$
Formula weight	522.17	450.10	477.17
Wavelength (Å)	0.71073	0.71073	0.71073
Crystal system	Monoclinic	Orthorhombic	Tetragonal
Space group	*C*2/*m*	*Ccca*	*P*4/*ncc*
a (Å)	9.0953(12)	8.4560(17)	8.7803(2)
b (Å)	8.9896(16)	10.426(2)	8.7803(2)
c (Å)	7.9046(13)	9.525(2)	15.5826(7)
β (deg)	92.212(10)		
Volume (Å^3)	645.82(18)	839.7(3)	1201.32(7)
Z	2	4	4
Density calculated (mg/m^3)	2.685	3.560	2.639
Absorption coefficient (mm^{-1})	12.638	19.375	10.241
F(000)	480	800	868
Temperature (K)	273(2)	273(2)	100(4)
Theta range for data collection	2.58–30.27 °	3.77–28.88 °	2.61–32.10 °
Index ranges	$-12\leqslant h\leqslant 11$, $-12\leqslant k\leqslant 12$, $-11\leqslant l\leqslant 11$	$-10\leqslant h\leqslant 11$, $-13\leqslant k\leqslant 13$, $-12\leqslant l\leqslant 12$	$-13\leqslant h\leqslant 13$, $-13\leqslant k\leqslant 12$, $-23\leqslant l\leqslant 23$
Reflections collected	3894	2959	24136
Independent reflections	944 [*R*(int) = 0.0601]	519 [*R*(int) = 0.0530]	1062 [*R*(int) = 0.0562]
Completeness to theta	Theta = 30.27 °/92.5%	Theta = 28.88°/92.7%	Theta = 32.10°/99.9%
Refinement method	Full-matrix least squares on F^2		
Data/restraints/parameters	944/0/44[a] *944/0/46*[b]	519/0/37	1062/0/42
Goodness-of-fit on F^2	1.189[a] *1.171*[b]	0.884	1.216
Final *R* indices [*I*>2sigma(*I*)], *R*1/w*R*2	0.0584, 0.1654[a] *0.0583*, *0.1626*[b]	0.0365, 0.0970	0.0382, 0.1002
R indices (all data), *R*1/w*R*2	0.0584, 0.1654[a] *0.0583*, *0.1626*[b]	0.0488, 0.1045	0.0641, 0.1117
Largest diff. peak/hole	5.735/−2.952 e Å^{-3}[a] *5.685/−3.046* e Å^{-3}[b]	1.719/−1.276 e Å^{-3}	2.219/−1.686 e Å^{-3}

[a] Values corresponding to the refinement of four water molecules.
[b] Values corresponding to the refinement of six water molecules.

Table 2
Atomic coordinates, equivalent isotropic and anisotropic displacement parameters[a] (Å^2) for $[U(C_2O_4)_2]\cdot 6H_2O$ (**1**)

	Site	*x*	*y*	*z*	*U* (eq)[b]
U	2*a*	0	0	0	0.0172(4)
C	8*j*	0.255(2)	0.247(2)	0.099(2)	0.051(4)
O(1)	8*j*	0.174(2)	0.162(2)	0.171(2)	0.059(4)
O(2)	8*j*	0.352(3)	0.333(3)	0.163(2)	0.103(9)
Ow1	4*g*	1/2	0.217(2)	1/2	0.057(5)
Ow2	4*i*	0.284(2)	0	0.514(2)	0.055(5)
Ow3	2*b*	0	1/2	0	0.77(11)[c]
Ow4	2*c*	0	0	1/2	0.74(11)[c]

	U^{11}	U^{22}	U^{33}	U^{23}	U^{13}	U^{12}
U	0.0159(5)	0.0141(4)	0.0215(5)	0	−0.0011(3)	0
C	0.050(11)	0.058(11)	0.044(8)	0.005(8)	−0.002(7)	−0.015(9)
O(1)	0.066(10)	0.073(10)	0.037(6)	0.008(6)	0.000(6)	−0.018(8)
O(2)	0.127(19)	0.150(20)	0.038(7)	0.000(9)	−0.012(9)	−0.084(17)
Ow1	0.086(16)	0.036(9)	0.045(9)	0	0.005(9)	0
Ow2	0.042(11)	0.078(14)	0.045(9)	0	0.004(8)	0

[a] The anisotropic displacement factor exponent takes the form: $-2\pi^2[h^2a^{*2}U^{11}+\cdots+2hka^*b^*U^{12}]$.
[b] *U*(eq) is defined as one-third of the trace of the orthogonalized U^{ij} tensor.
[c] Isotropic displacement parameter. The large values are discussed in the text.

sample was deposited on an alumina holder. Several diagrams were recorded between ambient temperature and 600 °C.

Thermogravimetric (TG) analysis was also carried out under argon flow at a constant rate of 2 °C/min up to 700 °C with a NETZSCH STA 409C analyzer. Evolving gases were examined by a SRA Instrument MTI.M200 μ-CPG. Using the same procedure, solid intermediates were isolated at specific temperatures for immediate structural characterizations.

For the initial, intermediate and final solid samples, UV–Vis and IR spectra were recorded between 400 and 800 nm with a HITACHI U-3000 analyzer equipped with an integration sphere and in the range 600–4000 cm^{-1} with a Bruker Equinoxe 55 Fourier Transform Infrared Spectrometer equipped with a Golden Gate diamond ATR reflection unit, respectively.

Scanning electron microscopic (SEM) observation was conducted with a FEI Quanta 200 microscope.

Table 3
Atomic coordinates, equivalent isotropic and anisotropic displacement parameters[a] (Å^2) for $[U(C_2O_4)_2 \cdot 2H_2O]$ (**2**)

	Site	x	y	z	U(eq)[b]
U	4*a*	0	1/4	1/4	0.0161(4)
C	16*i*	0.2908(13)	0.3086(12)	0.4687(13)	0.023(2)
O(1)	16*i*	0.2354(9)	0.3464(8)	0.3516(8)	0.021(2)
O(2)	16*i*	0.4032(14)	0.3539(11)	0.5327(12)	0.055(4)
Ow1	8*f*	0	0.0108(14)	1/4	0.050(4)

	U^{11}	U^{22}	U^{33}	U^{23}	U^{13}	U^{12}
U	0.0139(4)	0.0220(5)	0.0123(4)	0	0	0
C	0.013(5)	0.026(6)	0.029(6)	0.004(5)	−0.008(4)	−0.003(4)
O(1)	0.006(3)	0.033(4)	0.022(4)	0.009(3)	−0.009(3)	−0.010(3)
O(2)	0.057(7)	0.053(6)	0.055(7)	0.037(6)	−0.049(6)	−0.041(6)
Ow1	0.072(11)	0.021(6)	0.058(9)	0	0.044(9)	0

[a] The anisotropic displacement factor exponent takes the form $-2\pi^2[h^2a^{*2}U^{11} + \cdots + 2hka^*b^*U^{12}]$.
[b] U(eq) is defined as one-third of the trace of the orthogonalized U^{ij} tensor.

Table 4
Atomic coordinates and equivalent isotropic and anisotropic displacement parameters[a] (Å^2) for $[U(C_2O_4)_2 \cdot H_2O](C_2NH_7)$ (**3**)

	Site	x	y	z	U(eq)[b]
U	4*c*	1/4	1/4	0.45999(3)	0.0224(2)
C(1)	16*g*	0.4773(8)	−0.0409(8)	0.4592(4)	0.019(1)
O(1)	16*g*	0.3820(6)	0.0217(6)	0.4108(3)	0.026(1)
O(2)	16*g*	0.3327(6)	0.4612(5)	0.5548(3)	0.024(1)
Ow1	4*c*	1/4	1/4	0.3066(7)	0.031(2)
C(2)	16*g*[d]	−0.0250(17)	0.2555(17)	0.2256(8)	0.026(2)[c]
N(1)	8*f*[e]	−0.150(3)	0.350(3)	1/4	0.040(9)[c]
N(2)	8*f*[e]	−0.170(5)	0.170(5)	1/4	0.068(14)[c]

	U^{11}	U^{22}	U^{33}	U^{23}	U^{13}	U^{12}
U	0.0172(2)	0.0172(2)	0.0327(3)	0	0	0
C(1)	0.013(3)	0.018(3)	0.027(3)	−0.001(2)	−0.002(2)	0.000(2)
Ow1	0.032(3)	0.032(3)	0.030(4)	0	0	0
O(1)	0.027(3)	0.020(2)	0.031(2)	−0.006(2)	−0.009(2)	0.008(2)
O(2)	0.017(2)	0.020(2)	0.035(2)	−0.004(2)	0.009(2)	−0.006(2)
Ow1	0.032(3)	0.032(3)	0.030(4)	0	0	0

[a] The anisotropic displacement factor exponent takes the form $-2\pi^2[h^2a^{*2}U^{11} + \cdots + 2hka^*b^*U^{12}]$.
[b] U(eq) is defined as one-third of the trace of the orthogonalized U^{ij} tensor.
[c] Isotropic displacement parameter.
[d] Occupancy 0.5.
[e] Occupancy 0.25.

3. Results and discussion

The powder X-ray diffraction (PXRD) pattern of **1** is in agreement with that published by Jenkins et al. [24] (PDF 19-1379). It is completely indexed using the monoclinic symmetry and refinement of the unit cell parameters gives $a = 9.084(1)$, $b = 8.979(1)$, $c = 7.884(1)$ Å and $\beta = 92.20(1)^\circ$ (Fig. 2a). The actual monoclinic cell is related to the previously proposed triclinic one by the transformation matrix (1/2,1/2,0; 1/2,–1/2,0; 0,0,1). These results confirm the values calculated by Grigoriev et al. [26] assuming that both neptunium and uranium hexa-hydrated oxalates are isostructural. Refinement from the PXRD pattern (Fig. 2b) of the unit cell parameters gives $a = 8.5449(8)$, $b = 10.494(7)$ and $c = 9.419(8)$ Å for **2** in agreement with the previously reported results [24,25] (PDF 22-0961).

The crystal structure of the three compounds is built from the same type of two-dimensional metal organic framework resulting of the packing of four-membered rings $[U(C_2O_4)]_4$ which are formed by four uranium atoms connected through bis-chelating oxalate ions (Fig. 3a). In **1** the oxalate ions are perpendicular to the uranium plane leading to a planar layer and a distorted cubic environment of the uranium atom (Fig. 4a). The neutral $^2_\infty[U(C_2O_4)_2]$ layers are stacked along the [001] direction and the water molecules are located in the interlayer space (Fig. 3d). In **2**, the oxalate molecules are tilted approximately 45° compared to the uranium plane (Fig. 3b) allowing the rotation of about 45° of one face of the UO_8 cube, giving a square anti-prism. In this polyhedron the two square faces are closer together, the distance between the two planes becomes 2.08 Å instead of 2.64 Å in **1**, and the O atoms of the squares move away to allow a water oxygen to integrate the coordination sphere of uranium on each side and leads to a ten coordination of the U atom and to a bi-capped square anti-prism polyhedron (Fig. 4b). The U–OH_2 bonds are perpendicular to the mean plane of the uranium oxalates sheet. The neutral $^2_\infty[U(C_2O_4)_2 \cdot 2H_2O]$ layers are stacked along [001], two successive layers being translated of **a**/2 in such a way that one water molecule of a layer is above the hole on the preceding layer. The empty interlayer space is reduced and the distance between the mean planes of successive layers highly decreases from 7.905(1) Å in **1** to 5.213(1) Å in **2**. In **3**, only one water oxygen enters the coordination sphere of the uranium atom, so the coordination number is nine and the coordination polyhedron can

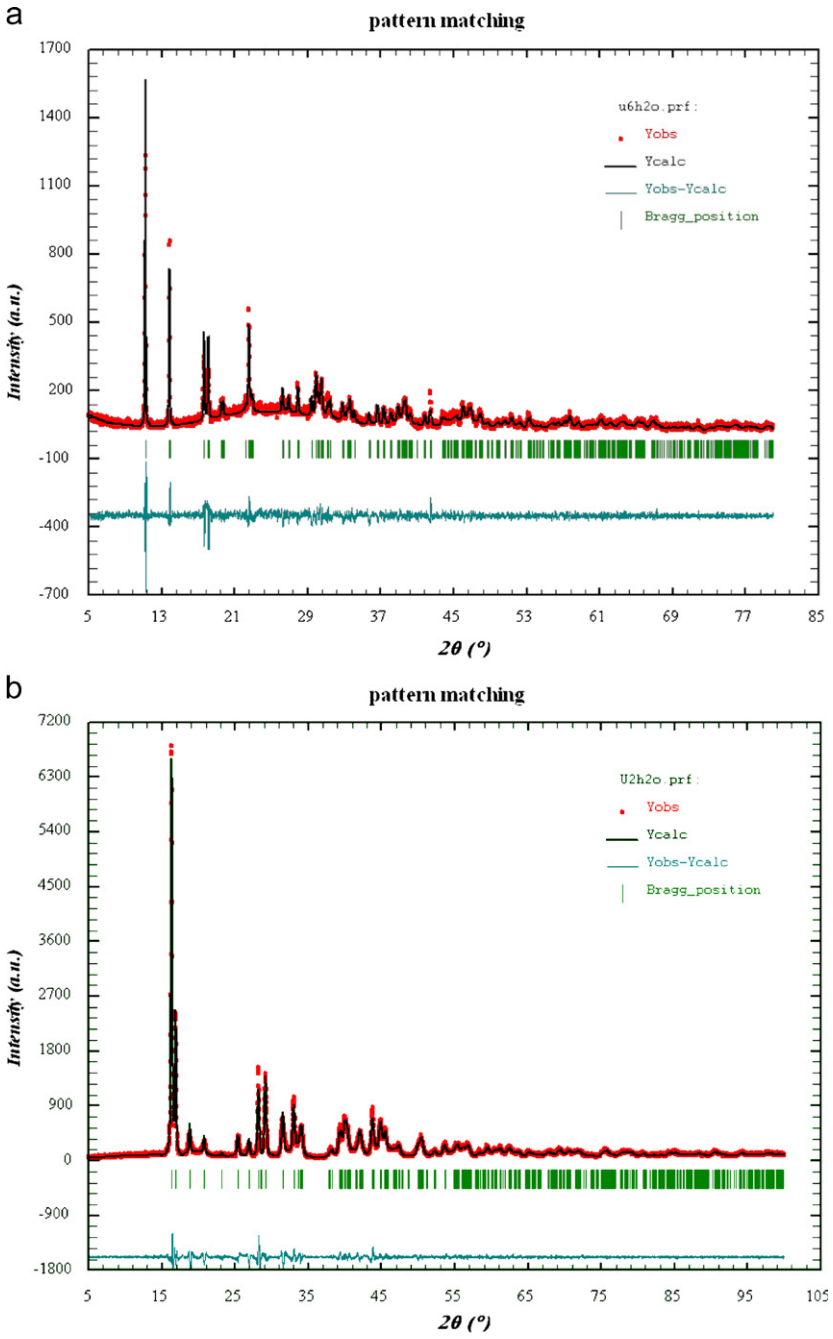

Fig. 2. PXRD pattern and corresponding pattern matching refinement of (a) $U(C_2O_4)_2 \cdot 6H_2O$ and (b) $U(C_2O_4)_2 \cdot 2H_2O$.

be described as a distorted square anti-prism mono-capped by the water oxygen atom (Fig. 4c) with an intermediate value of the distance between the two square planes (2.24 Å). The uranium atom is not anymore at the centre of the polyhedron but is moved towards the water oxygen atom. The water oxygen atoms are alternately above and below the mean plane so a corrugated layer is obtained. The organic molecules are located between the neutral layers stacked along [001] (Fig. 3f). One can reasonably imagine that the same type of layer could exist in the monohydrated uranium oxalate $U(C_2O_4)_2 \cdot H_2O$. In fact, this layer is similar to that found in various yttrium or lanthanide oxalates with interlayer monovalent ions to compensate the negative charge of the lanthanide oxalate layer, $NH_4[Ln(C_2O_4)_2 \cdot H_2O]$ obtained for Ln = Y, Eu–Yb [36,37], $Na[Y(C_2O_4)_2 \cdot H_2O] \cdot 3H_2O$ [38], $Na[Yb(C_2O_4)_2(H_2O)] \cdot 3H_2O$ [23], $Cs[Y(C_2O_4)_2 \cdot H_2O]$ [39], $(CN_3H_6)[La(C_2O_4)_2 \cdot H_2O]$ and $(NH_4)_{0.5}(CN_3H_6)_{0.5}[Nd(C_2O_4)_2 \cdot H_2O]$ [40] and in the quadratic series of oxalates with U(IV)/Ln(III) mixed site recently reported [23]. The monohydrated uranium oxalate $[U(C_2O_4)_2 \cdot H_2O]$ and $NH_4[Ln(C_2O_4)_2 \cdot H_2O]$ could be the limits of this quadratic series formulated $(NH_4)_{1-x}[U_{1-x}Ln_x(C_2O_4)_2 \cdot H_2O] \cdot nH_2O$ obtained for various lanthanides and some values of x [41].

The reported compounds are the first examples of two-dimensional network of U(IV) and oxalate ions and illustrate the versatility of the U(IV) environment with a coordination number varying from 8 to 9 and 10. In fact the flexibility of the metal organic arrangement and rotations of the oxalate ions allow a distortion and a breathing of the uranium polyhedron that, starting from a slightly distorted cube with oxygen from four oxalates as vertices, can accept, after a 45° rotation of one face,

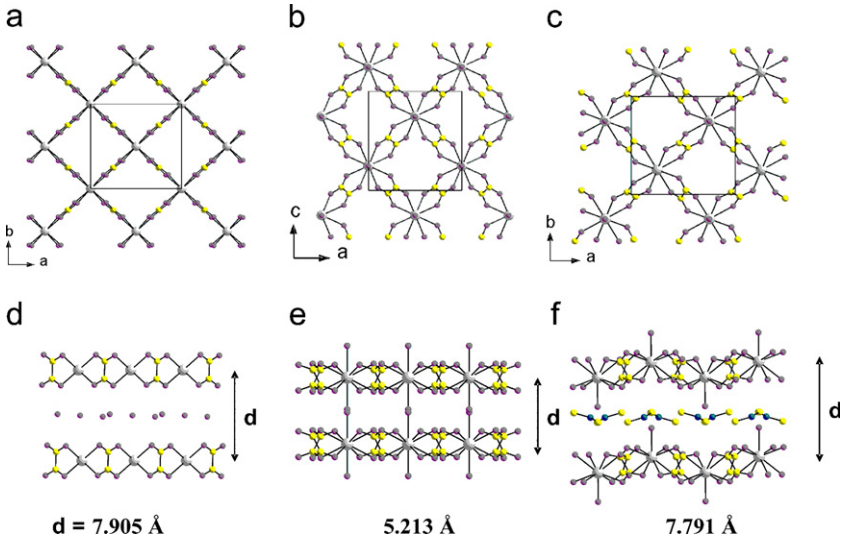

Fig. 3. The two-dimensional neutral $^{2}_{\infty}[U(C_2O_4)_2]$ metal organic framework resulting of uranium atoms connected through bis-chelating oxalate ions to form four-membered rings $[U(C_2O_4)]_4$ in $U(C_2O_4)_2 \cdot 6H_2O$ (a). In $[U(C_2O_4)_2 \cdot H_2O](C_2NH_5)$ and $U(C_2O_4)_2 \cdot 2H_2O$, the deformation of the uranium-oxalate arrangement and the modification of the uranium environment allowing the addition of one and two oxygen water atoms, respectively, to create neutral $^{2}_{\infty}[U(C_2O_4)_2 \cdot H_2O]$ (c) and $^{2}_{\infty}[U(C_2O_4)_2 \cdot 2H_2O]$ (b) metal organic framework. In $U(C_2O_4)_2 \cdot 6H_2O$ and $[U(C_2O_4)_2 \cdot H_2O](C_2NH_7)$ the uranium oxalate layers are stacked one above the other and the water (d) or solvate molecules (f) occupy the interlayer space. On the contrary in $U(C_2O_4)_2 \cdot 2H_2O$, successive $^{2}_{\infty}[U(C_2O_4)_2 \cdot 2H_2O]$ layers are translated in a such a way that water oxygen atoms of a layer belong to the vertical of the centers of square holes of the two surrounding layers (e).

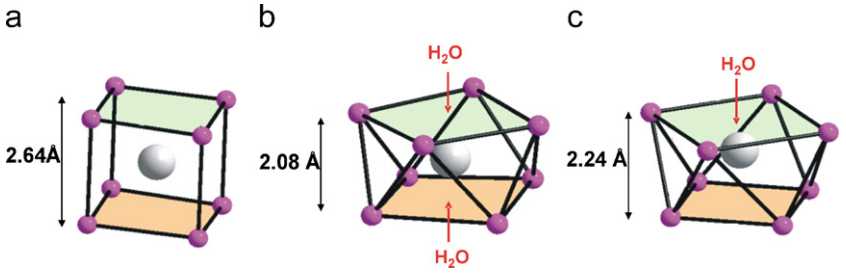

Fig. 4. The coordination of U(IV) ion in $U(C_2O_4)_2 \cdot 6H_2O$ by eight oxygen atoms from four oxalate ions to form a distorted cubic environment (a). In $U(C_2O_4)_2 \cdot 2H_2O$, the tilt of the uranium atoms—oxalate ions flexible network leads to an anti-prism polyhedron around the uranium atom which is completed by two water oxygen atoms that capped the squared faces (b). In the solvated monohydrated uranium oxalate $[U(C_2O_4)_2 \cdot H_2O](C_2NH_7)$, the antiprism is capped only on one side by a water oxygen atom (c).

Table 5
The U(IV) containing oxalates reported up today with the coordination number for the U(IV) atom, the average U–O distance, the valence bond sum (v) for U^{4+}, the dimensionality of the arrangement (D) of the uranium structural block units (SBU)

Compound	CN	〈U–O〉	v	D	SBU	Ref.
$U(C_2O_4)_2 \cdot 6H_2O$	8	2.48(2)	3.08	2D	$[U(C_2O_4)_4]$	This work
$U(C_2O_4)_2 \cdot 1H_2O$, C_2NH_7	9	2.452(6)	3.60	2D	$[U(C_2O_4)_4 \cdot H_2O]$	This work
$Ba_2U(C_2O_4)_4 \cdot 8H_2O$	9	2.407(4)	4.11	0D	$[U(C_2O_4)_4 \cdot H_2O]$	[18]
$K_2MnU(C_2O_4)_4 \cdot 9H_2O$	9	2.42(4)	3.97	0D	$[U(C_2O_4)_4 \cdot H_2O]$	[19]
$K_2CdU(C_2O_4)_4$	9	2.42(1)	3.93	0D	$[U(C_2O_4)_4 \cdot H_2O]$	[20]
$K_2Mg_2U_2(C_2O_4)_7 \cdot 11H_2O$	10	2.465(7)	3.90	1D	$[U(C_2O_4)_5]$	[20,38]
$K_4U(C_2O_4)_4 \cdot 4H_2O$ ortho	10	2.45(1)	4.04	1D	$[U(C_2O_4)_5]$	[17]
$K_4U(C_2O_4)_4 \cdot 4H_2O$ tricl	10	2.467(5)	3.89	1D	$[U(C_2O_4)_5]$	[17]
$U(C_2O_4)_2 \cdot 2H_2O$	10	2.461(11)	3.90	2D	$[U(C_2O_4)_4 \cdot 2H_2O]$	This work
$(NH_4)_2U_2(C_2O_4)_5 \cdot 0.7H_2O$	10	2.461(13)	3.90	3D	$[U(C_2O_4)_5]$	[21]

one or two supplementary water oxygen atoms. Table 5 reports the different U(IV) containing oxalates reported till today with the characteristics of the U(IV) coordination. In this family of compounds, no eight-coordinated U(IV) was previously reported. The cubic coordination is rarely found in complexes for which the more commonly found geometries are square anti-prism and dodecahedron. However, this coordination exists in oxides such as UO_2 with fluorite-type structure and a perfect cubic environment of the U(IV) ions with a U–O distance of 2.368 Å. In the previously reported U(IV) oxalates with four oxalate bidentate ligands around U(IV), $Ba_2U(C_2O_4)_4 \cdot 8H_2O$ [18], $K_2CdU(C_2O_4)_4$ [17] and $K_2MnU(C_2O_4)_4 \cdot 7H_2O$ [19], the oxalates are tetrahedrally arranged (Fig. 5a), the coordination being completed by a water oxygen to give a tri-capped trigonal prism rather than a mono-capped square anti-prism. In fact the squares of such a coordination polyhedron are formed by oxygen atoms from two oxalate ions. The $[U(C_2O_4)_4 \cdot H_2O]$ entities are not connected directly but through the divalent metals (Ba, Cd, Mn) to give a 3D-arrangement. On the contrary, in the present compounds, the four oxalate ions are tetragonally arranged around U(IV), the four oxygen

atoms of the squares belong to four different oxalate ions that are shared with four other U(IV) given rise to a 2D-arrangement and eight-, nine- or ten-coordinated U(IV) depending the number of water oxygen that capped the square prism or anti-prism (Fig. 5b–f). To our knowledge, it is the first example of ten-coordinated U(IV) by four chelating oxalates and two water oxygen. In the so far reported U(IV) oxalates with ten-coordinated U(IV), the coordination polyhedron is formed by oxygen atoms from five chelating oxalates adopting two configurations. The first one (Fig. 5g) allows the connection of the $[U(C_2O_4)_5]$ unit blocks through trans oxalates to create one-dimensional arrangement in $K_4U(C_2O_4)_4 \cdot 4H_2O$ [17] (Fig. 5i). Two parallel chains can further share a third bi-chelating oxalate to build double chains ribbon in $K_2Mg_2U_2(C_2O_4)_7 \cdot 11H_2O$ [20,42] (Fig. 5j). In the second configuration the five oxalates form a trigonal bipyramid around U(IV) (Fig. 5h), the $[U(C_2O_4)_5]$ unit blocks sharing their three equatorial oxalate ions to form a honeycomb-like hexagonal rings (Fig. 5k), further pillared by the apical oxalate ions to build a three-dimensional porous framework [21]. The average U–O distances are comparable in all the oxalate compounds with ten coordinated uranium atoms whatever the geometry of the polyhedron and, in **2**, the valence bond sum is in agreement with the theoretical one (+4). Astonishingly, the decrease of the coordination number of uranium from 10 to 9 and 8 in compounds **2** to **3** and **1**, respectively is not accompanied by a decrease of the average U–O distance and, as a result, the bond valence sums indicate an under-bonding of the uranium atom and lead for **1** to an unexpected calculated valence of +3. While the U–O (oxalate) distances are comparable in the three compounds, the U–O (water) distance is significantly shorter in **3** than in **2** (Table 6), which is even shorter than in other oxalates where this distance is close to 2.55 Å.

Compound **1** is isostructural with the neptunium analogue [26]. As in the hexa-hydrated neptunium oxalate, only four water oxygen atoms, instead of six, are unambiguously localized from the X-ray single crystal structure determination in the interlayer space in two sites. There is an available (2*b*) site, as indicated by the PLATON software, to accommodate a water molecule. The introduction of this Ow3 water oxygen atom in the refinement gives an unacceptable value of the corresponding atomic displacement parameter $U = 0.57(9)\,Å^3$! This site is localized at the center on the uranium–oxalate square cycle, the oxygen atom being surrounded by 16 oxalate oxygen atoms (Fig. 6a) (4O(1) at

Table 6
Uranium–oxygen distances in for $[U(C_2O_4)_2] \cdot 6H_2O$, **1** $[U(C_2O_4)_2 \cdot 2H_2O]$, **2** and $[U(C_2O_4)_2 \cdot H_2O](C_2NH_7)$, **3**

	1	2	3
U–O(1)	2.509(15) (4 ×)	2.431(7) (4 ×)	2.439(5) (4 ×)
U–O(2)	2.426(19) (4 ×)	2.475(9) (4 ×)	2.479(5) (4 ×)
U–Ow1		2.494(15) (2 ×)	2.390(10) (1 ×)
〈U–O〉	2.467(17)	2.461(12)	2.452(6)

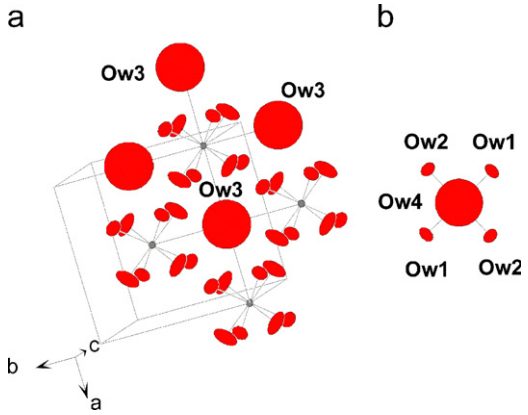

Fig. 6. The environment of supplementary water oxygen atoms Ow3, by 16 oxalate oxygen atoms at too long distances (a), and Ow4 by four water oxygen atoms at too short distances (b), in $U(C_2O_4)_2 \cdot 6H_2O$.

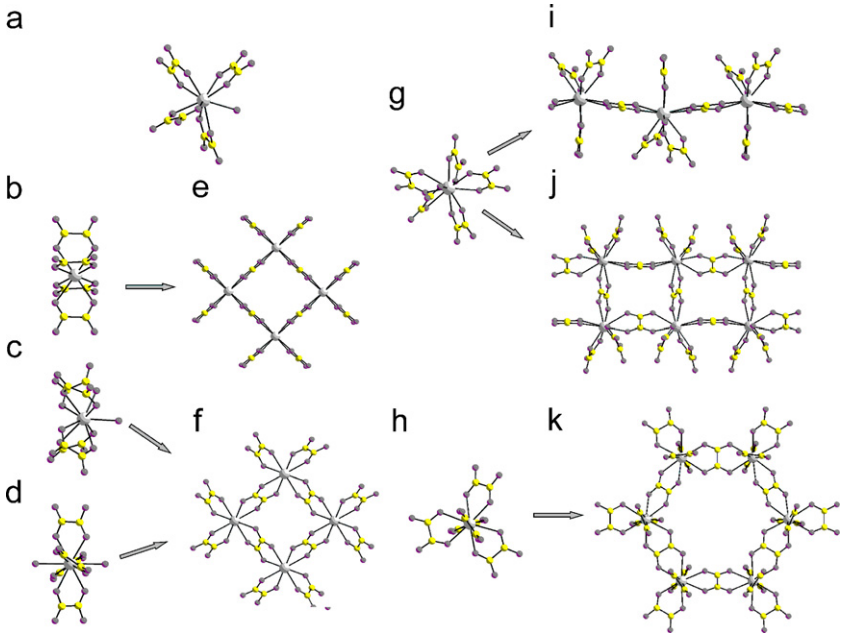

Fig. 5. The tetragonal arrangement of the four oxalate ligands around U(IV) in $U(C_2O_4)_2 \cdot 6H_2O$ (b) allows the formation of a bi-dimensional arrangement of four-membered rings (e), the introduction of one (c) or two (d) water oxygen atoms in the coordination polyhedron, in $U(C_2O_4) \cdot H_2O.(C_2NH_5)$ and $U(C_2O_4) \cdot 2H_2O$, respectively, does not prevent this formation of a bi-dimensional arrangement (f). On the contrary, for a tetrahedral arrangement of the four oxalate ligands around U(IV), a bi-dimensional arrangement is not created and the $[U(C_2O_4)_4 \cdot H_2O]^{4-}$ ions are isolated (a). For ten-coordinated U(IV) by five bidentate oxalates, two geometries (g and h) are observed that lead to one-dimensional (i and j) or three-dimensional (k) arrangements.

3.61(2)Å, 4O(1) at 3.66(2)Å, 4O(2) at 3.54(3)Å and 4O(2) at 3.73(3)Å) at too long distances to correspond to hydrogen bonds, thus this oxygen atom must be moved towards one or two atoms and, as a result, being delocalized on several sites of higher multiplicity, which could explain the high value of the atomic displacement parameter. Finally, another water molecule can be localized in the interlayer space in the (2*c*) site, the corresponding refined atomic displacement parameter is also too large and equal to that of Ow3 when the two atoms are introduced in the refinement. This Ow4 atom is surrounded by four water oxygen (two Ow1 and two Ow2) forming a square (Fig. 6b) at too short distances for hydrogen bonds and must be moved away from the square plane and, consequently, partially occupy sites of higher multiplicity. As the uranium atom is heavy and there are experimental difficulties in obtaining better crystals, these disorders of course cannot be taken into account.

The TGA and DTA curves (Fig. 7a) and the DXHT plots (Fig. 7c) of the hexa-hydrated uranium (IV) oxalate decomposition in air show that the dehydration starts at very low temperature—in fact the XRD at 40 °C shows both the hexa- and dehydrate—and proceeds in three successive stages to the anhydrous oxalate $U(C_2O_4)_2$ through the dihydrate and the monohydrate. The oxalate decomposition starts during the last dehydration as evidenced by the formation of CO_2 at about 200 °C (Fig. 7b), leading to amorphous UO_3 further reduced at 550 °C into crystallized U_3O_8.

Under argon atmosphere, the dehydration proceeds through the same steps (Fig. 8a). Unlike the behavior in air, decomposition of anhydrous oxalate proceeds through the formation of an oxy-carbonate in agreement with the results of Zhirov [43], the CO_2/CO ratio (Fig. 8b) (3/4) corresponding to the formation of $UO_{1.5}(CO_3)_{0.5}$. The oxy-carbonate slowly decomposes into UO_2.

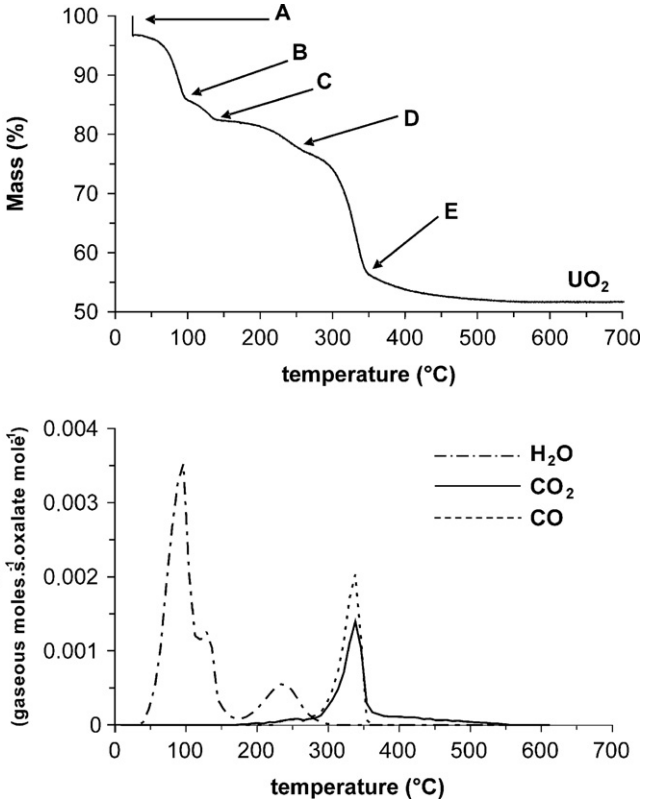

Fig. 8. TG curve (a) and evolved gas analysis by μ-CPG (b) during $U(C_2O_4)_2 \cdot 6H_2O$ decomposition under an argon flow (A: $U(C_2O_4)_2 \cdot 6H_2O$, B: $U(C_2O_4)_2 \cdot 2H_2O$, C: $U(C_2O_4)_2 \cdot H_2O$, D: $U(C_2O_4)_2$ and E: $UO_{1.5}(CO_3)_{0.5}$).

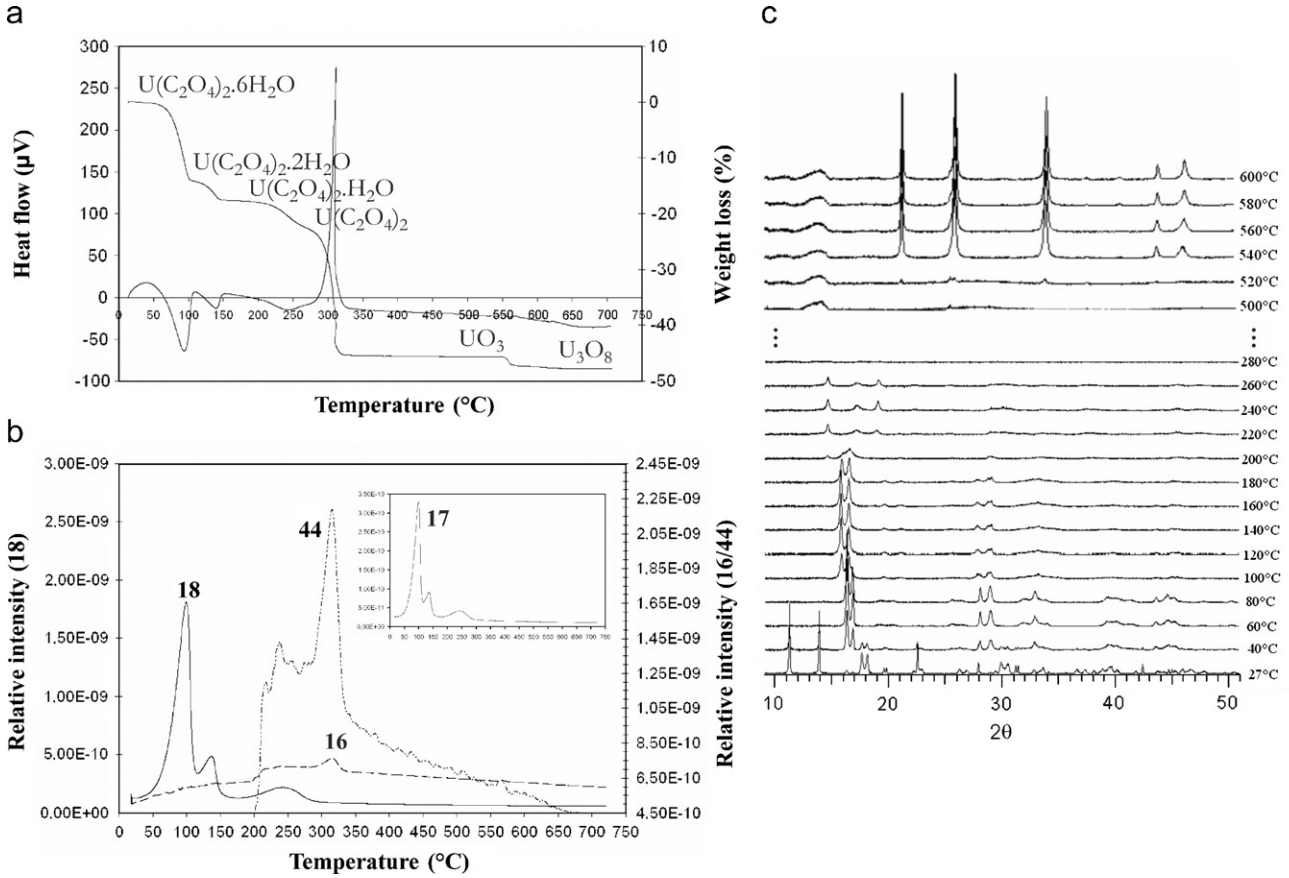

Fig. 7. $U(C_2O_4)_2 \cdot 6H_2O$ thermal analyses under a N_2–O_2 gas atmosphere (N_2:O_2 = 4:1 by vol) (a) TGA and DTA curves, (b) MS analysis of the evolved H_2O and CO_2 and (c) HTXRD plot at various temperatures (the hump at low angle observed at higher temperature is due to the sample holder).

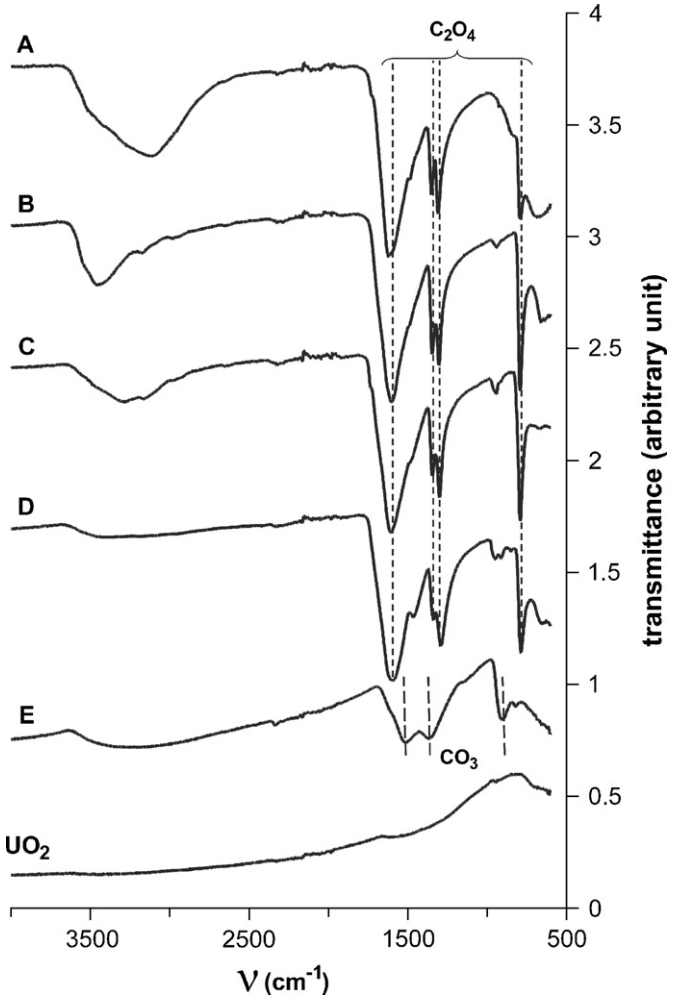

Fig. 9. Comparison of the infrared spectra of the initial and intermediate samples during the $U(C_2O_4)_2 \cdot 6H_2O$ thermal decomposition under an argon flow (A: $U(C_2O_4)_2 \cdot 6H_2O$, B: $U(C_2O_4)_2 \cdot 2H_2O$, C: $U(C_2O_4)_2 \cdot H_2O$, D: $U(C_2O_4)_2$ and E: $UO_{1.5}(CO_3)_{0.5}$).

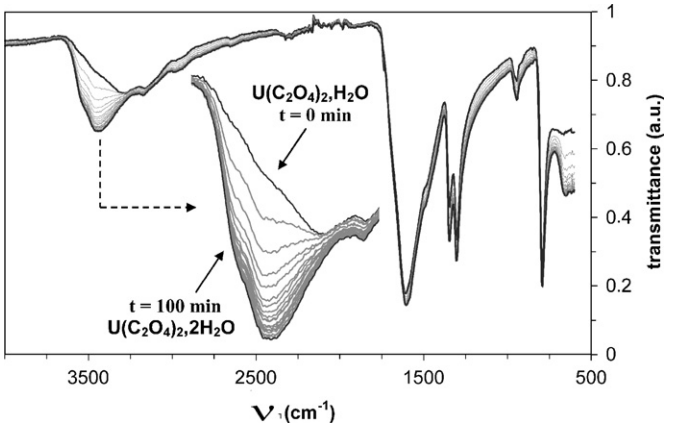

Fig. 10. Infrared spectra during rehydration of the $U(C_2O_4)_2 \cdot H_2O$ into $U(C_2O_4)_2 \cdot 2H_2O$ showing the shift of the H_2O band.

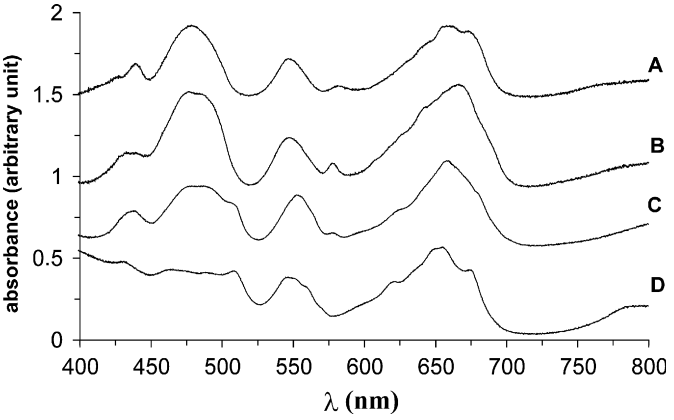

Fig. 11. UV–Vis spectra of the intermediate products of the $U(C_2O_4)_2 \cdot 6H_2O$ decomposition under argon flow (A: $U(C_2O_4)_2 \cdot 6H_2O$, B: $U(C_2O_4)_2 \cdot 2H_2O$, C: $U(C_2O_4)_2 \cdot H_2O$, D: $U(C_2O_4)_2$ and E: $UO_{1.5}(CO_3)_{0.5}$).

The infrared spectra for compounds A ($U(C_2O_4)_2 \cdot 6H_2O$), B ($U(C_2O_4)_2 \cdot 2H_2O$), C ($U(C_2O_4)_2 \cdot H_2O$) and D ($U(C_2O_4)_2$) corresponding to the initial sample and to the samples heated at 105, 155, 275 °C, respectively, are compared in Fig. 9. In the four spectra, the oxalate bands are present practically at the same positions (1590, 1490, 1355, 1315 and 795 cm^{-1}). For the sample heated at 350 °C (E) these bands disappear and are replaced by the characteristic bands of the carbonate ion (at 1535, 1370 and 910 cm^{-1}). For the first compound, the water molecules appear as a broad band between 3635 and 2570 cm^{-1}; on the contrary, for B, a less broad band centred at 3450 cm^{-1} is present, finally the band is shifted to lower frequencies in the monohydrate. The displacement and change of form of this band transduce the different role of the water molecules in the three compounds. Fig. 10 shows the modification of infrared spectrum of C, recorded every 5 min, during the re-hydration of the monohydrate to the dihydrate compound, at 27.5 °C under air with a water content of 54%, showing the shift of the water band. Direct UV–Vis spectra on the solids shown in Fig. 11 highlight the stability of the U(IV) during the dehydration, which is opposite to the corresponding Pu(IV) oxalate thermal decomposition, for which intermediate reduction into Pu(III) oxalate $Pu_2(C_2O_4)_3$ has been recently evidenced [44]. SEM observations show that the morphology of the oxalate precursor that appear as square plates (Fig. 12a and b) are preserved on calcination into UO_2 (Fig. 12d and e) and that during the first step of dehydration the square plate crystals have a tendency to delaminate in (001) planes (Fig. 12c). That corresponds to the escape of water molecules along the (001) plane in the crystal. This delamination allows further escape of CO_2 and CO in this plane and explains the preservation of the particles morphology upon calcination to UO_2.

4. Conclusion

Due to the very low solubility of U(IV) oxalates, single crystals are difficult to obtain and, in spite of the importance of theses compounds in the nuclear fuel technology and in waste decontamination, their structures remained unknown. The use of hydrothermal conditions allows us to prepare crystals of the uranium (IV) oxalate hexahydrate and dihydrate, and, using ions diffusion through a TEOS gel, crystals of the monohydrate form solvated with dimethylamine were obtained. Despite poor quality and instability of hexahydrate crystals, and the actual disorder of some water molecules, the structure has been satisfactorily described in the monoclinic cell and is at least sufficiently informative to allow a structural discussion of the modifications during the dehydration process. The three structures are built on a two-dimensional supramolecular edifice of uranium (IV) connected through oxalate ions. The distortion of this porous edifice during the transitions allows important modification of the coordination polyhedra of the uranium atoms which, starting

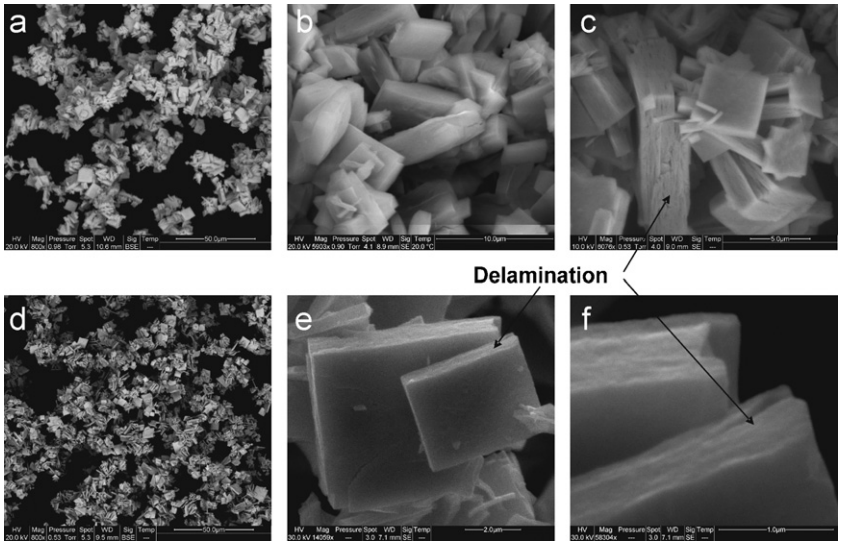

Fig. 12. Scanning electron microscopy micrograph of the uranium (IV) oxalate (a and b), the square plate-like particles delaminate during the first step of dehydration (c). The particle shape is preserved upon calcination into uranium dioxide (d) which are also delaminated in the initial (001) plane of the oxalate precursor (e and f).

with an unexpected cube of eight oxygen atoms from four oxalate ions in the hexahydrate, inserts two water oxygen atoms and one water oxygen atom for the dihydrate and the monohydrate, respectively. These results clearly point out the adaptability of the coordination of uranium (IV) and allows us to envisage a very rich structural chemistry for this atom whose oxidation state's not well studied.

Acknowledgments

This research was financially supported by AREVA NC, France. We thank Jean Luc Emin, AREVA NC, France, for encouraging this work and for fruitful discussions.

References

[1] D. Ferri, M Iuliano, C. Manfredi, E. Vasca, T. caruso, M. Clemente, C. Fontanella, J. Chem. Soc. Dalton Trans. (2000) 3460.
[2] E.E. Baeva, Yu.N. Mikhailov, Yu.E. Gorbunova, L.B. Serezhkina, V.N. Serezhkin, Russ. J. Inorg. Chem. 47 (9) (2002) 1348.
[3] E.E. Baeva, Yu.N. Mikhailov, Yu.E. Gorbunova, L.B. Serezhkina, V.N. Serezhkin, Russ. J. Inorg. Chem. 48 (11) (2003) 1651.
[4] N.W. Alcock, J. Chem. Soc. Dalton Trans. (1973) 1610.
[5] N.W. Alcock, J. Chem. Soc. Dalton Trans. (1973) 1614.
[6] N.W. Alcock, J. Chem. Soc. Dalton Trans. (1973) 1616.
[7] N.C. Jayadevan, K.D. Singh Mudher, D.M. Chackraburtty, Acta Crystallogr. B 31 (1975) 2277.
[8] N.C. Jayadevan, D.M. Chackraburtty, Acta Crystallogr. B 28 (1972) 3178.
[9] J.P. Legros, Y. Jeannin, Acta Crystallogr. B 32 (1976) 2497.
[10] S. Govindarajan, K.C. Patil, D.M. Poojary, H. Manohar, Inorg. Chim. Acta 120 (1986) 103.
[11] M.D. Poojary, K.C. Patil, Proc. Indian Acad. Sci. 99 (5&6) (1987) 311.
[12] M. Yu. Artem'eva, Yu.N. Mikhailov, Yu.E. Gorbunova, L.B. Serezhkina, V.N. Serezhkin, Zh. Neorg. Khim. 48 (9) (2003) 1473.
[13] B. Chapelet-Arab, G. Nowogrocki, F. Abraham, S. Grandjean, Radiochim. Acta 93 (2005) 279.
[14] L. Duvieubourg, G. Nowogrocki, F. Abraham, S. Grandjean, J. Solid State Chem. 178 (2005) 3437.
[15] P.A. Giesting, N.J. Porter, P.C. Burns, Z. Kristallogr. 221 (2006) 252.
[16] P. Thuéry, Polyhedron 26 (2007) 101.
[17] M.C. Favas, D.L. Kepert, J.M. Patrick, A.H. White, J. Chem. Soc. Dalton Trans. (1983) 571.
[18] M.R. Spirlet, J. Rebizant, Acta Crystallogr. C 43 (1987) 19.
[19] K.P. Mörtl, J.-P. Sutter, S. Golhen, L. Ouahab, O. Kahn, Inorg. Chem. 39 (2000) 1626.
[20] I. Imaz, G. Bravic, J.P. Sutter, J. Chem. Soc. Dalton Trans. (2005) 2681.
[21] B. Chapelet-Arab, G. Nowogrocki, F. Abraham, S. Grandjean, J. Solid State Chem. 178 (2005) 3046.
[22] B. Chapelet-Arab, G. Nowogrocki, F. Abraham, S. Grandjean, J. Solid State Chem. 178 (2005) 3055.
[23] B. Chapelet-Arab, L. Duvieubourg, G. Nowogrocki, F. Abraham, S. Grandjean, J. Solid State Chem. 179 (2006) 4003.
[24] I.L. Jenkins, F.H. Moore, M.J. Waterman, J. Inorg. Nucl. Chem. 27 (1965) 77.
[25] R. Bressat, B. Claudel, Y. Trambouze, J. Chim. Phys. 60 (1963) 1265.
[26] M.S. Grigor'ev, I.A. Charushnikova, N.N. Krot, A.I. Yanovskii, Yu.T. Struchkov, Radiochemistry 39 (1997) 420.
[27] V.A. Golovnya, G.T. Bolotova, Russ. J. Inorg. Chem. 9 (1964) 155.
[28] V.I. Spitsyn, K.M. Dunaeva, A.V. Dubrovin, A.I. Zhirov, N.A. Santalova, G.N. Mazo, Russ. J. Inorg. Chem. 25 (1980) 15.
[29] Bruker Analytical X-ray system, SAINT+, Version 6.22, Madison, USA, 2001.
[30] G. M Sheldrick, SHELXTL NT, Program Suite for Solution and Refinement of Crystal Structure, version 5.1, Bruker Analytical X-ray Systems, 1998.
[31] G.M. Scheldrick, SADABS, Bruker-Siemens Area Detector Absorption and Other Correction, version 2.03, 2001.
[32] H.M. Rietveld, Acta Crystallogr. 22 (1967) 151.
[33] H.M. Rietveld, Acta Crystallogr. 25 (1992) 589.
[34] J. Rodrigez Carvajal, M.T. Fernandez Diaz, J.L. Martinez, J. Phys.: Condens. Matter 3 (1991) 3215.
[35] C. Caglioti, A. Paoletti, E.P. Ricci, Nucl. Instrum. Methods 3 (1958) 223.
[36] T.R.R. McDonald, J.M. Spink, Acta Crystallogr. 23 (1967) 944.
[37] J.-C. Trombe, P. Thomas, C. Brouca-Cabarrecq, Solid State Sci. 3 (2001) 309.
[38] T. Bataille, D. Louër, Acta Crystallogr. C 55 (1999) 1760.
[39] T. Bataille, J.-P. Auffredic, D. Louër, J. Mater. Chem. 10 (2000) 1707.
[40] F. Fourcade-Cavaillou, J.-C. Trombe, Solid State Sci. 4 (2002) 1199.
[41] B. Arab-Chapelet, S. Grandjean, G. Nowogrocki, F. Abraham, J. Nuclear Mater. 373 (2008) 259.
[42] I. Imaz, G. Bravic, J.P. Sutter, Chem. Commun. (2005) 993.
[43] A.I. Zhirov, K.M. Dunaeva, R.R. Khudyakova, Sov. Radiochem. (2005) 993.
[44] N. Vigier, S. Grandjean, B. Chapelet-Arab, F. Abraham, J. Alloys Compds. 444–445 (2007) 594.